Am J Cancer Res 2024;14(5):2538-2554
www.ajcr.us /ISSN:2156-6976/ajcr0155552

Original Article

KIF2C is a critical regulator for malignant progression of head and neck squamous cell carcinoma

Haiyue Zhu[1,2,3*], Yuxin Bao[1,2,3*], Xuanqi Dou[2,3*], Xiaofeng Zuo[2,3], Junhong Ye[2,3], Haiyu Ma[1,2,3], Youquan Bu[2,3], Yitao Wang[2,3], Jiang Zhu[1,3]

[1]Department of Otolaryngology, The First Affiliated Hospital of Chongqing Medical University, Chongqing Medical University, Chongqing 400016, P. R. China; [2]Department of Biochemistry and Molecular Biology, College of Basic Medical Sciences, Chongqing Medical University, Chongqing 400016, P. R. China; [3]Molecular Medicine and Cancer Research Center, Chongqing Medical University, Chongqing 400016, P. R. China. [*]Equal contributors.

Received January 21, 2024; Accepted May 8, 2024; Epub May 15, 2024; Published May 30, 2024

Abstract: Head and neck squamous cell carcinoma (HNSCC) is a significant cause of mortality, while the underlying mechanism remains unclear. Our studies have revealed that KIF2C plays a crucial role in tumor proliferation and metastasis in HNSCC. The results demonstrate that KIF2C is highly expressed at both the mRNA and protein levels and is closely associated with lymph node metastasis. The gene ontology and Kyoto Encyclopedia of Genes and Genomes pathway analyses indicate that the differentially expressed genes are enriched in processes or pathways related to cell adhesion and cell mitosis in HNSCC. Moreover, the established protein-protein interaction network identifies KIF2C as a potential hub gene in HNSCC. Knockdown of KIF2C has been demonstrated to significantly reduce cell migration and invasion ability, leading to cell cycle arrest, a high proportion of abnormal cell apoptosis, and cell chromosome division mismatches in the HNSCC cell line. Downstream genes such as PDGFA, EGFR, TP63, SNAI2, KRT5, and KRT14 were found to be down-regulated, and multiple critical pathways, including mTOR, ERK, and PI3K-AKT pathways, were inactivated as a result of KIF2C knockdown. These findings provide strong evidence for the crucial role of KIF2C in HNSCC and suggest that targeting KIF2C may be a promising therapeutic strategy for this disease. Knockdown of KIF2C has been shown to significantly inhibit tumor proliferation in nude mice, demonstrating the potential therapeutic role of KIF2C in HNSCC treatment.

Keywords: Head and neck cancer, KIF2C, metastasis, cell cycle, proliferation

Introduction

Head and neck squamous cell carcinoma (HNSCC) is the seventh most common cancer globally, with 1.1 million new cases and 4.1 million existing cases annually, accounting for 4.9% of new cancer cases and 4.7% of cancer-related deaths worldwide [1-3]. Recent epidemiological research indicates a gradual increase in the incidence of HNSCC, which may be associated with the prevalence of HPV infection [4, 5]. And more and more patients are being diagnosed with advanced head and neck cancer. Patients with advanced head and neck cancer face obstacles in HNSCC treatment, including metastasis, ineffective treatment, and drug resistance [6]. The eighth edition of the AJCC Cancer Staging Manual recommends that patients with terminal HNSCC utilize a Combination of treatments, including surgery, radiation therapy, targeted therapy and immunotherapy [7, 8]. Ongoing combination therapy trials utilizing platinum, docetaxel, cetuximab, targeted therapy and immune checkpoint inhibitors have shown some progress [9]. Therefore, there is an urgent need for molecular mechanistic research on HNSCC to explore novel medication combinations, enhance efficacy, and reduce toxicity, in order to develop combination regimens with better efficacy and fewer adverse effects for advanced patients with HNSCC [9].

Kinesin family member 2C (KIF2C), also referred to as MCAK, is a member of the kinesin-13 family. KIF2C is localized to microtubules was confirmed to regulate microtubule dynamic instability, triggering catastrophic depolymerization [10-19]. KIF2C facilitates the swift disas-

https://doi.org/10.62347/CIBM2965

sembly of microtubules through a conformational alteration. Dysregulation of its function can result in severe chromosomal instability and mitotic defects [20-22]. Recently, it has been reported that KIF2C is overexpressed in primary breast, lung, and oral cancer tissues [23-29]. There is also a similar upregulation of mRNA expression levels of KIF2C in HNSCC. There is a notable correlation between the expression of KIF2C and the grade, stage, and prognosis of patients. However, the specific function of KIF2C in HNSCC has not yet been determined.

The objective of our study was to identify the differentially expressed genes of HNSCC. These genes were then used for GO and KEGG pathway analysis, as well as for constructing protein-protein interaction networks. Our results indicate that cell-cell adhesion and cell mitosis are critical events in the tumorigenesis of HNSCC. Among the key genes implicated in HNSCC development, KIF2C is an essential hub regulator. Our study confirms that KIF2C plays a regulatory role in the malignant phenotype of HNSCC cells. Therefore, KIF2C represents a novel therapeutic target for HNSCC treatment.

Material and methods

Analyze the differentially expressed genes of HNSCC

RNA-seq and clinical data for patients with Head and neck squamous cell carcinoma were acquired through the Cancer Genome Atlas (TCGA) data portal (https://xenabrowser.net/). The dataset includes 43 pairs of adjacent non-tumor tissue samples and tumor tissue samples and 460 unpaired tumor samples. 34 discrete samples were excluded through cluster analysis, and finally 512 samples were used for subsequent analysis. Duplicate genes and genes without corresponding annotation information in the expression matrix data were filtered out prior to analysis. The expression matrix data were analyzed using the R package DESeq2. Differentially expressed genes (DEGs) were selected based on the false discovery rate were below 0.05 and gene expression fold change above 2 (|FC|>2).

Gene enrichment analysis

DEGs were used for GO annotation and KEGG pathway enrichment analysis by using the R package. P<0.05 was defined as the cut-off criterion to search out significant biological processes (BP) of GO and KEGG pathway enrichment terms. Some significant terms were presented as the bar chart which was conducted by ggplot2 package in R.

Protein-protein interaction network

Protein-protein interactions were conducted by using the STRING online website (https://string-db.org/). The parameters for the analysis were set using a fold change in gene expression higher than 2 and a minimum connection score threshold of 0.4. Then protein-protein interaction data was imported into Cytoscape3.8.2 software to plot the interaction network. Finally, the MCODE plugin was utilised to identify the most significant genes. 12 crucial hub genes were identified with the most protein-protein interactions in the network.

KIF2C knockdown stable cell line construction

Two types of HNSCC cell lines, specifically FaDu (human hypopharynx squamous cell carcinoma) and SCC15 (human tongue squamous cell carcinoma), were acquired from the Chinese Academy of Sciences Shanghai cell bank in Shanghai, China. FaDu cells were cultivated using MEM/EBSS (Hyclone), while SCC15 cells were cultured with DMEM (Gibico). Both media were supplemented with 1% penicillin-streptomycin (Solarbio) and 10% FBS (PAN). The cells were consistently cultured in an incubator at 37°C with 5% CO_2. The double-stranded negative control short hairpin RNA (shRNA) oligonucleotides and shRNA targeting human KIF2C mRNA labeled as NCsh and KIF2Csh in figures, were synthesized by Sangon (Sangon Biotech, Shanghai, China) and cloned into the AgeI/EcoRI sites of the pLKO.1-puro lentiviral vector (The sequences are shown in Table S1). The plasmids were described in our previous article [30]. The lentivirus particles were produced by co-transfection of the vectors of pLKO.1-puro, pSPAx2 and pMD2.G into 293T cells (human embryonic kidney cells), by Neofect DNA transfection reagent (Neofect, Beijing, China). Lentiviruses were used to infect HNSCC cells, and the cells were screened with puromycin (2 μg/ml) for 96 hours to obtain stable cell strains.

Quantitative real-time PCR and Western blotting

Total RNA was extracted using the Omega Bio-Tek RNA Isolation Kit I (Omega Bio-Tek), following the manufacturer's instructions. RNA purifi-

cation was achieved through a silica gel column, and the isolated RNA was then utilized to synthesize cDNA with SYBR Premix Ex Taq (Perfect Real Time, Takara), with GAPDH as the reference gene. The RT-PCR protocol was executed per previous illustration. Refer to Table S2 for primer details.

For the Western blot assay, the cells were lysised by sonication after addition of RIPA lysate buffer. Total cell lysates were subjected to SDS-PAGE gel electrophoresis and then transferred to a polyvinylidene fluoride (PVDF) transfer membrane and visualized by enhanced chemiluminescence (ECL) from Bio-Rad Laboratories (Hercules, CA, USA). The information of antibodies were supplemented in Table S3.

Cell viability assay and cell synchronization

Paclitaxel (PTX) is a conventional anti-tumor drug that induces mitotic arrest and apoptosis, ultimately leading to cell death. The PTX purchased from Aladdin was solubilized with DMSO. The experimental HNSCC cell lines were treated with a 10 nM concentration of PTX for 24 hours. To acquire mitosis images, the cells were treated with RO-3306 (Selleck Chemicals) to synchronize in the G2 phase. In brief, the medium was supplemented with RO-3306 at a final concentration of 9 mM for 20 hours. Afterwards, the cells were released from G2 phase for a duration of two hours. The effect of paclitaxel on cell growth was analyzed by using the Real-time Cell History Recorder (JULI Stage NanoEntek, Seoul, Korea).

Cell migration and wound-healing assay

Briefly, 5×10^4 cells were seeded into 6-well plates, after infected with lentiviral particles of NCsh and KIF2Csh for 48 h, and cells were cultured until at 95% confluence.

Cells were scratched and images were taken at 0, 24, 48 h for FaDu or at 0, 6, 12 h for SCC-15, using Leica light microscope (DM4B, Leica Corporation, Wetzlar, Germany). Cell motility was quantified using Image J and dead or split cells were excluded from the motility assay.

For cell motility assay, cells were collected and resuspended in 6-well plates with a concentration of 5×10^3 cells/mL. The images were taken continuously by JULI Stage Real-time Cell History Recorder (NanoEntek, Seoul, South Korea) for 8 h with an interval of 15 min.

The individual cell motility ability was quantified by Image-pro. Cells that were died, dividing or moved out of the vision were excluded for motility assessment.

Immunofluorescence assays

The exponentially growing cells fixed with 4% paraformaldehyde in 24-well plates at room temperature for 30 minutes. After permeabilized using 0.2% Triton X-100 for 15 minutes and submerged in 1.5% FBS/PBS for 30 minutes, the HNSCC cells were incubated with indicated primary antibodies and fluorescent secondary antibodies sequentially. The cell nuclei were stained with DAPI. The immunofluorescence images were acquired using confocal microscopy (LSM800 confocal microscope). Additional information regarding the antibodies can be found in Table S3.

Cell cycle and apoptosis assay

Cells were harvested via trypsin digestion and low-temperature centrifugation, then washed and fixed for staining. For cell cycle analysis, cells were fixed with 75% ethyl alcohol and subjected to analysis using FL2-A and PE-A. The Annexin V-FITC Apoptosis Detection Kit (BD Pharmingen, Franklin Lake, USA) was used to stain the cells with Annexin V-FITC phosphatidylserine (PS) and propidium iodide (PI). Technical abbreviations were explained upon first use. The cell cycle analysis and apoptosis assay were both detected using Fluorescence-Activated Cell Sorting.

RNA-sequencing analysis

Total RNA was extracted according to the instructions. The RNA is stored at a low temperature to prevent degradation. The next step involved constructing the cDNA library for DNBSEQ RNA-Seq. After filtering the raw data obtained from RNA sequencing, a total of 2228 genes exhibiting differential expression were identified based on the |FC|>2. Subsequently, KEGG pathways and gene enrichment analysis was conducted to identify pathways featuring distinct characteristic changes.

Tumor xenografts

BALB/c-nude mice (female, 5-6 weeks of age, weighing 18-20 g) were utilized for this study. To create the subcutaneous xenograft model, 1×10^6 FaDu cells were suspended in 100 μL PBS, then injected subcutaneously into the labeled nude mice's axillary. The injection site was checked for any instances of leakage or bleeding in the mice. The subcutaneous implant tumor in nude mice was measured every three days using a vernier caliper. Tumor volume was calculated using the equation $\pi \times L \times W^2/6$ (L = length, W = width). After four weeks, the mice were sacrificed in routine method, and the dissected tumor was weighed, plotted on statistical maps, and significance was calculated. No mice died during the experiment. The animal studies followed the CQMU animal care guidelines and were approved by the CQMU Institutional Animal Care and Usage Committee.

Statistical analysis

Statistical results were obtained through SPSS 16.0 software (SPSS statistical software Inc., Chicago, USA), while GraphPad Prism software (GraphPad Prism Software) was utilized for statistical analysis. Statistical significance was evaluated using Student's t-tests and log rank tests, with a significance level of $P<0.05$.

Results

Identification and functional enrichment analysis of DEGs in HNSCC

To gain insight into the molecular and cellular mechanisms of HNSCC, we first analyzed differentially expressed genes of HNSCC from The Cancer Genome Atlas database. The results showed that 1531 genes were down-regulated, while 1602 genes were up-regulated in the HNSCC samples compared to the normal samples (**Figure 1A**). GO and KEGG pathway enrichment analyses were conducted by using the DEGs. GO-BP enrichment analysis revealed that the DEGs in HNSCC were primarily implicated in cell adhesion, cell chemotaxis, cell mitotic nuclear division, and other cancer-associated biological processes (**Figure 1B** and Table S4). KEGG pathway analysis revealed that DEGs were not only associated with cell mobility and migration related pathways, but were also enriched in cell proliferation related pathways (**Figure 1C** and Table S5). These pathways include PI3K-Akt, and JAK-STAT signaling. Specifically, cell adhesion dysregulation is a critical event implicated in HNSCC tumorigenesis.

KIF2C-containing network is overexpressed in HNSCC

To identify key genes that may regulate the development of HNSCC, we constructed a protein-protein interaction network using the online tool STRING (**Figure 2A**). We identified the top 12 key DEGs as valuable hub genes in HNSCC, including KIF2C, BUB1B, CCNA2, CDCA8, CCNB2, CDC45, ASPM, MELK, AURKB, TTK, CDK1, and NCAPG (**Figure 2B**). These 12 hub genes are associated with the cell cycle, located in the core interaction network, and show a significant positive expression correlation with each other (**Figure 2C**).

It is worth noting that KIF2C and ASPM are also listed as key genes in our nasopharyngeal cancer study [30]. AURKB, BUB1B, CCNA2, and CDC45 were reported also associated with HNSCC, which supports the authenticity of the above PPI network [31-35]. These 12 key genes are expressed at significantly higher levels in tumor tissues than in normal tissues (**Figure 2D**). Correlation analysis between the KIF2C mRNA expression levels and TNM stage revealed that KIF2C were closely associated with the lymph node staging of HNSCC and were not correlated with T-stage, M-stage, and clinical grade (**Figure 2E**).

KIF2C knockdown inhibits HNSCC cell proliferation

To gain insight into the function of KIF2C in HNSCC, the expression of KIF2C of two HNSCC cell lines (FaFu and SCC15) was suppressed by using lentiviral system. KIF2C knockdown was confirmed via qRT-PCR and WB (**Figure 3A** and **3B**), which showed a significant decrease in mRNA and protein levels. Several phenotypic experiments were then constructed to determine the role of KIF2C in HNSCC cell lines. The results indicate that the morphology of the cell has been altered and cell proliferation slows down after KIF2C knockdown in FaDu and SCC-15 cells (**Figure 3C** and **3D**). These results indicate that KIF2C silencing inhibits the proliferation of the HNSCC cell lines.

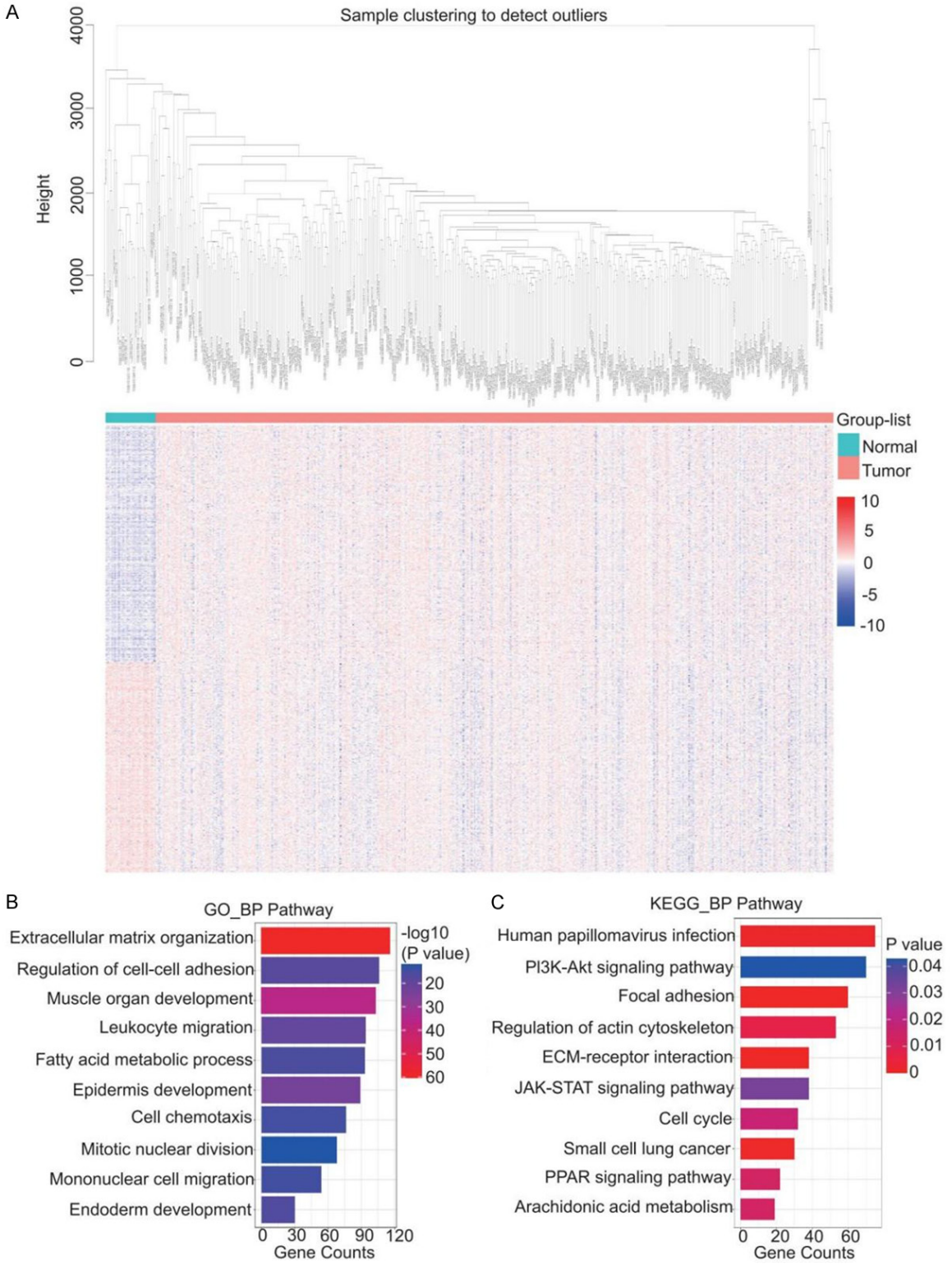

Figure 1. Identification and functional enrichment analysis of DEGs in HNSCC. A. Clustering of samples and heat map of differentially expressed genes in HNSCC. Blue-to-red linear gradient colors were associated with the indicated amount of gene expression. B. GO enrichment analysis of DEGs in HNSCC, only gene-enriched biological processes are shown. C. KEGG pathway analysis of DEGs in HNSCC.

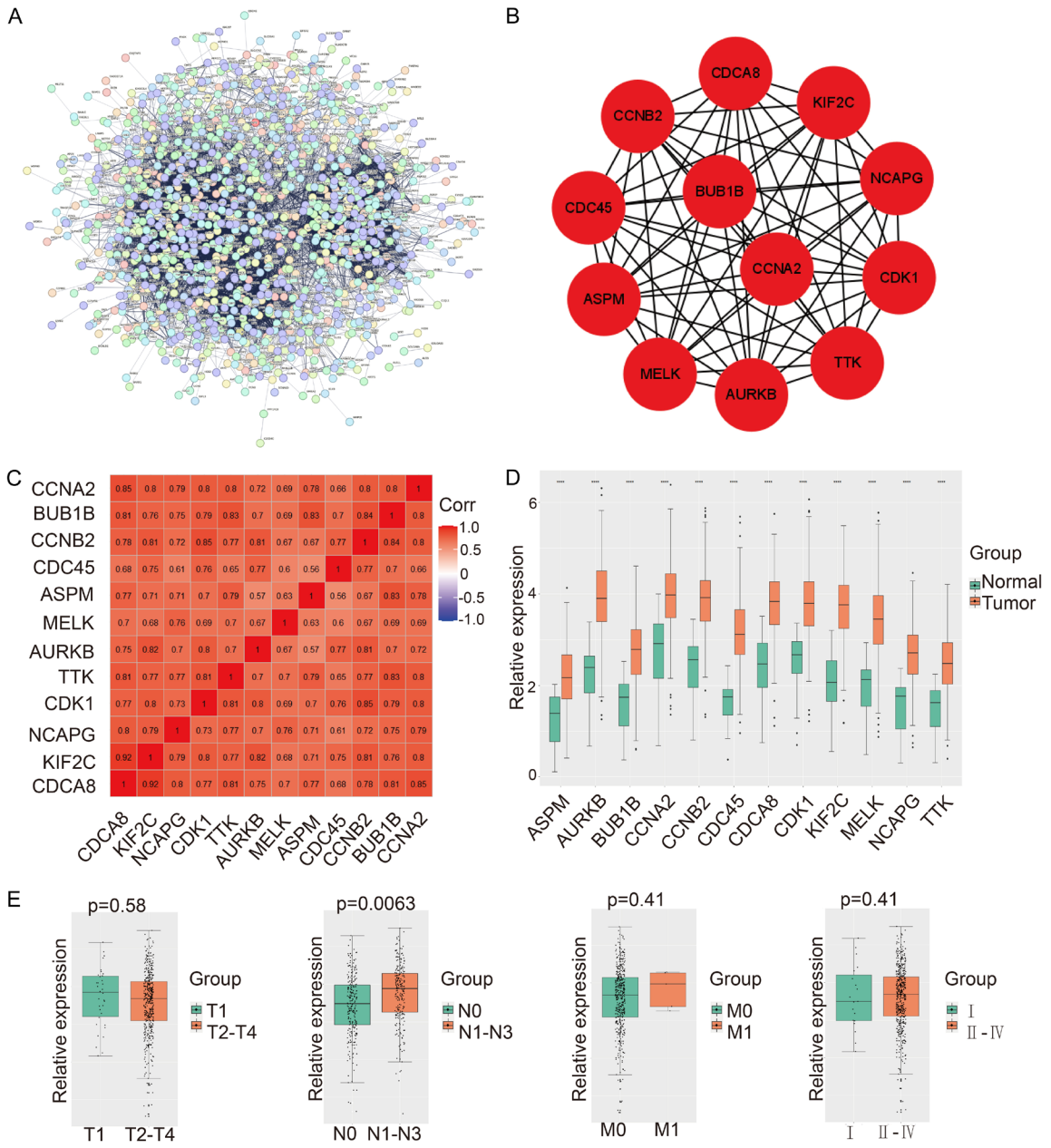

Figure 2. KIF2C-containing network is overexpressed in HNSCC. A. PPI network of DEGs in HNSCC. B. The core PPI network containing top 12 key hub DEGs. KIF2C, BUB1B, CCNA2, CDCA8, CCNB2, CDC45, ASPM, MELK, AURKB, TTK, CDK1, and NCAPG. C. Correlation analysis of the 12 key genes. D. mRNA expression levels of 12 key genes in HNSCC. E. KIF2C showed significantly associated with different lymph node stages in HNSCC. According to the 8th edition of the AJCC (2018), "T1" represents stage T1 in T-staging, and "T2-T3" includes patients with stage T2 and T3; "N0" represents patient without regional lymph node metastasis, and "N1-N3" represents patients with metastasis in either lymph node; "M0" and "M1" are the M-stages; "I" patients at stage T1 without lymph node metastasis or distant metastasis, and "II-IV" patients with T-stage greater than T1 or any metastasis.

KIF2C knockdown induces HNSCC cell cycle arrest and apoptosis

To investigate whether KIF2C regulates the cell cycle and apoptosis of HNSCC cells, flow cytometry was used to analyze cell cycle and apoptosis after KIF2C knockdown. The results showed a significant arrest in cell cycle progression in the KIF2C knockdown group. Specifically, the proportion of cells in the G1 phase decreased by 9.6% and those in the S phase increased by 7.1% compared to the negative control cells. In

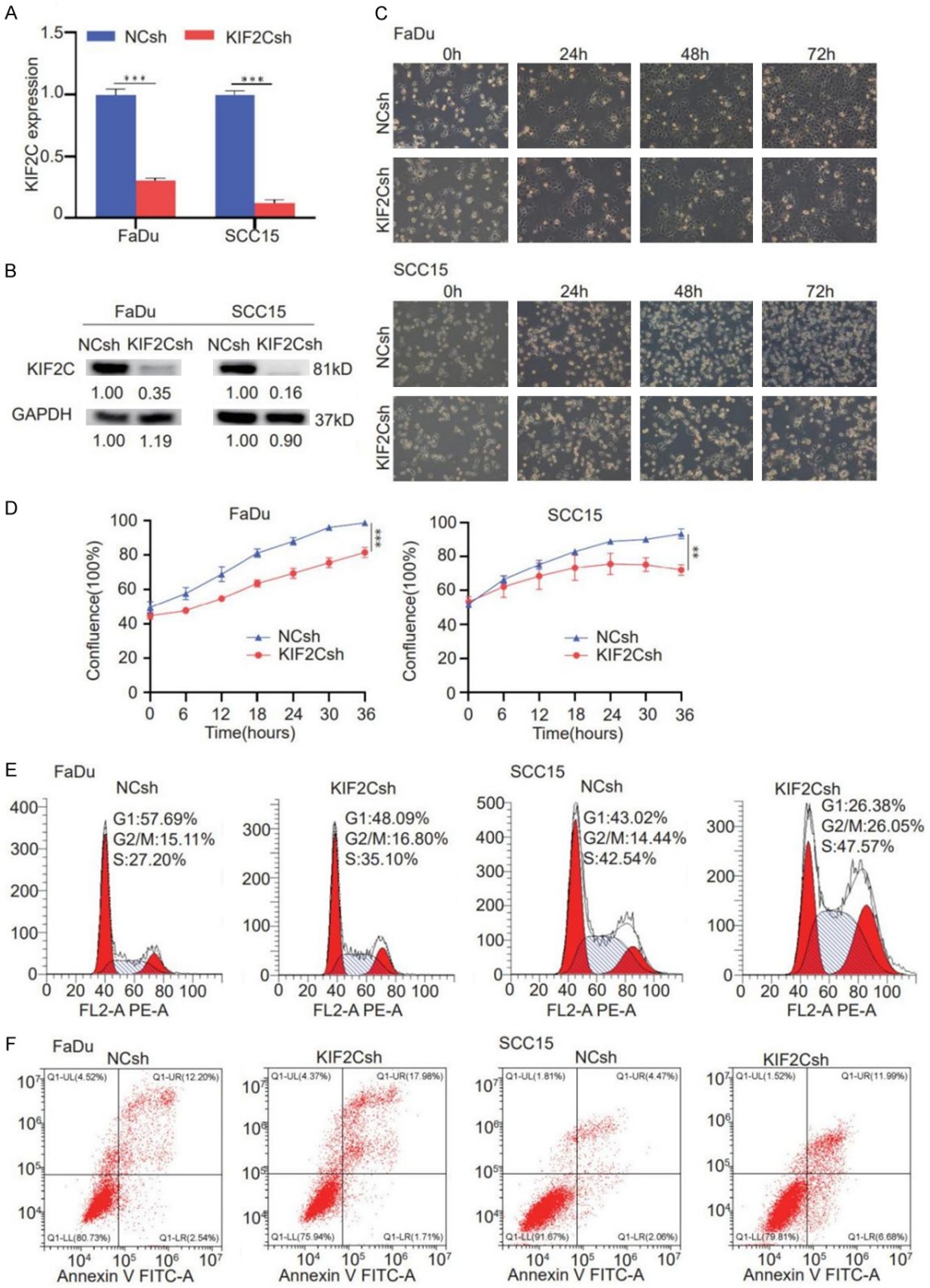

Figure 3. The knockdown of KIF2C inhibits the HNSCC cell proliferative capacity. A, B. The mRNA protein levels of KIF2C was significantly decreased after KIF2C knockdown in HNSCC cell (FaDu and SCC15). B. KIF2C knockdown influenced the morphology of HNSCC cells (100×). C, D. The growth of KIF2C knockdown cells was observed by Leica light microscope (DM4B, Leica Corporation, Wetzlar, Germany) every 6 h for 48 h. Scale bars, 200 μm. E, F. Cell cycle and apoptosis of FaDu and SCC15 cells infected lentivirus-KIF2C shRNA and lentivirus-negative control were analyzed by flow cytometry.

KIF2C-knockdown SCC15 cells, the proportion of cells in G1 phase decreased from 43.02% to 26.38% compared to the corresponding control groups. Additionally, the percentage of cells in G2/M phase increased by 16.64% in KIF2C knockdown SCC15 cells compared to the control group (**Figure 3E**). The results of the cell apoptosis assay indicate that knocking down KIF2C in FaDu cells led to a higher percentage (17.98%) of late apoptotic cells after 48 hours of cultivation compared to only 12.20% in the negative control group. Similarly, KIF2C knockdown in SCC15 cells resulted in early and late apoptotic cells at roughly 6.68% and 11.99%, respectively, while the control group showed only 2.06% and 4.47% (**Figure 3F**). Collectively, these results suggest that reducing KIF2C expression could lead to cell arrest and apoptosis in HNSCC.

KIF2C knockdown decreases HNSCC cell migration

The Functional Enrichment Analysis of DEGs revealed that dysregulation of cell adhesion is a crucial event implicated in HNSCC tumorigenesis. Dysregulation of cell adhesion is linked to cell metastasis. To assess changes in the migratory capabilities of tumor cells after KIF2C knockdown, cell motility was measured using the Real-time Cell History Recorder. Our experiment on wound healing showed that cells infected with NC shRNA migrated faster than KIF2C knockdown cells in both FaDu and SCC15 (**Figure 4A** and **4B**). Additionally, single cell motility analysis revealed that cells exhibited disordered movement, and the average running distance and moving velocity decreased upon KIF2C knockdown in HNSCC cells (**Figure 4C** and **4D**). Taken together, these experimental findings demonstrate that KIF2C plays a significant role in regulating the mobility of HNSCC cells.

KIF2C knockdown causes mitotic defects in HNSCC cells

Based on preliminary exploratory findings on the regulatory role of KIF2C in tumors, we conducted immunofluorescence to investigate its regulatory role in HNSCC cells during the mitotic phase. Our immunofluorescence results demonstrate a significant increase in abnormal multi-nucleated cell numbers after KIF2C knockdown (**Figure 5A** and **5B**). Furthermore, the immunofluorescence images confirm that knockdown of KIF2C results in defects in mitotic spindle formation and abnormal chromosome assembly, as observed through a confocal microscope. Specifically, the hairy spindle exhibited aberrant spindles with longer microtubules and disorganized astral microtubules, while the central spindle microtubules were also more disordered (**Figure 5C** and **5D**). Our analysis suggests that the dysfunction of microtubule depolymerization, caused by KIF2C knockdown, contributes to the observed mitotic defects in HNSCC cells.

KIF2C knockdown enhances paclitaxel sensitivity in HNSCC cells

Paclitaxel is often used to treat HNSCC because it enhances microtubule assembly while inhibiting microtubule depolymerization. This leads to the suppression of microtubule dynamics, which is relevant to KIF2C function. Therefore, this connection suggests that knockdown of KIF2C combined with paclitaxel may have a superior effect on inhibiting HNSCC cell proliferation. Our experiment demonstrated a significant alteration in cell morphology. After 24 hours of exposure to 10 nM paclitaxel in KIF2C knockdown cells, there was a noticeable increase in the number of cells becoming rounder and brighter (**Figure 6A** and **6B**). Meanwhile, KIF2C knockdown combined with paclitaxel in head and neck cancer cells showed a higher mortality rate in Taipan blue staining of cells (**Figure 6C**). Therefore, KIF2C knockdown enhances paclitaxel sensitivity in HNSCC cells.

Identification of downstream targeted genes and pathways regulated by KIF2C

To explore the intrinsic molecular mechanisms by which KIF2C promotes the malignant phenotype of HNSCC cells, we performed RNA-seq analyses to identify DEGs in KIF2C knockdown cells. 2,228 differentially expressed genes were identified after KIF2C knockdown, including 1,631 up-regulated genes and 597 down-regulated genes (**Figure 7A**).

These DEGs were enriched in cell adhesion, proliferation and chemotaxis (**Figure 7B** and Table S6). KEGG pathway analysis revealed that DEGs were enriched in cancer-related transcriptional dysregulation, cell adhesion, signal transduction and other pathways (**Figure 7C**

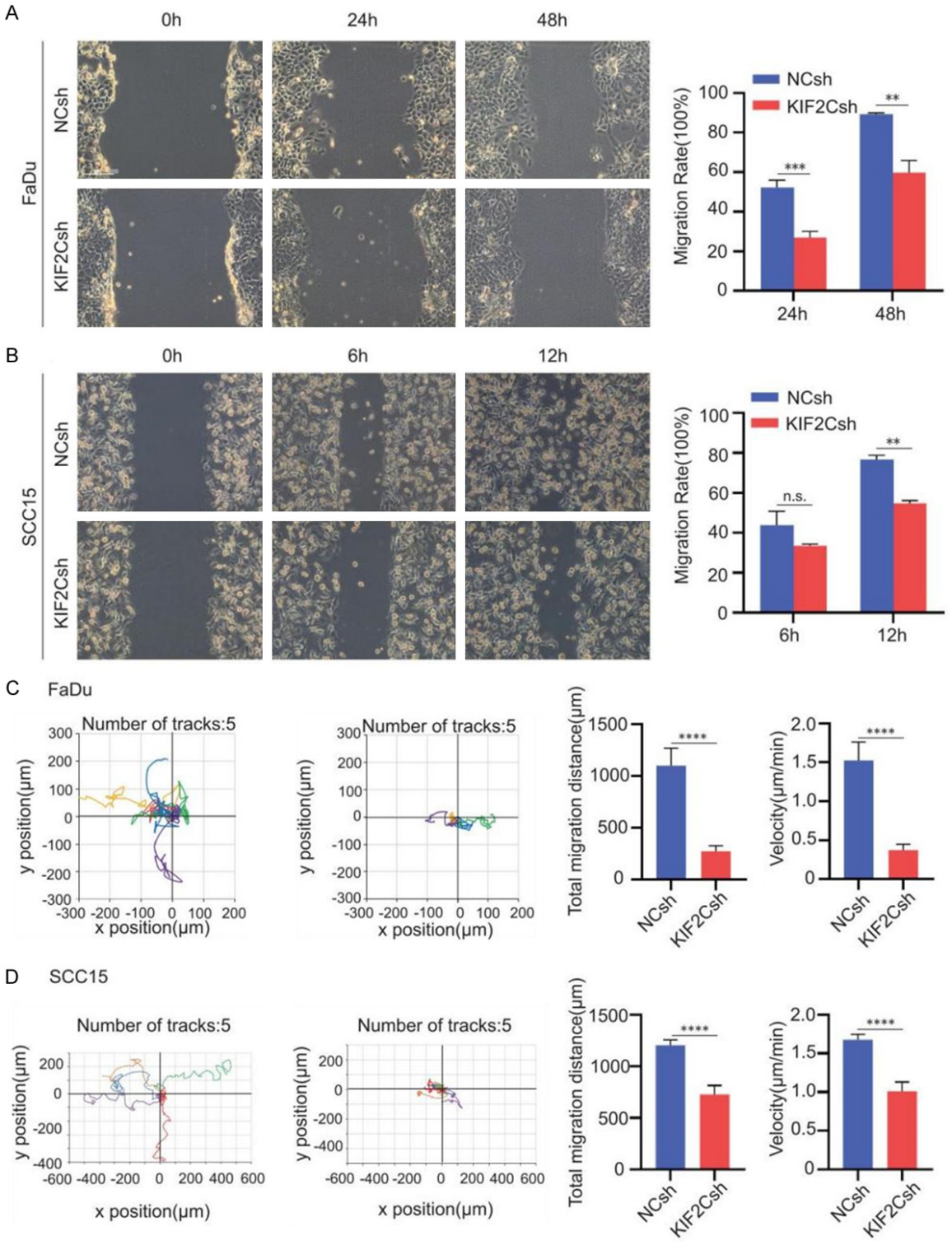

Figure 4. Migration and motility decreased in KIF2C knockdown HNSCC cell. A, B. Wound healing assay was conducted in FaDu and SCC15 cells infected with KIF2C shRNA and shNC lentivirus grewing for 48 h. Bar = 200 μm. C, D. Cell motilities of FaDu and SCC15 were monitored by cell history recorder mentioned every 15 min for 12 h. Motile trajectories of individual cell movement are presented and mean total migration distances and speeds are displayed.

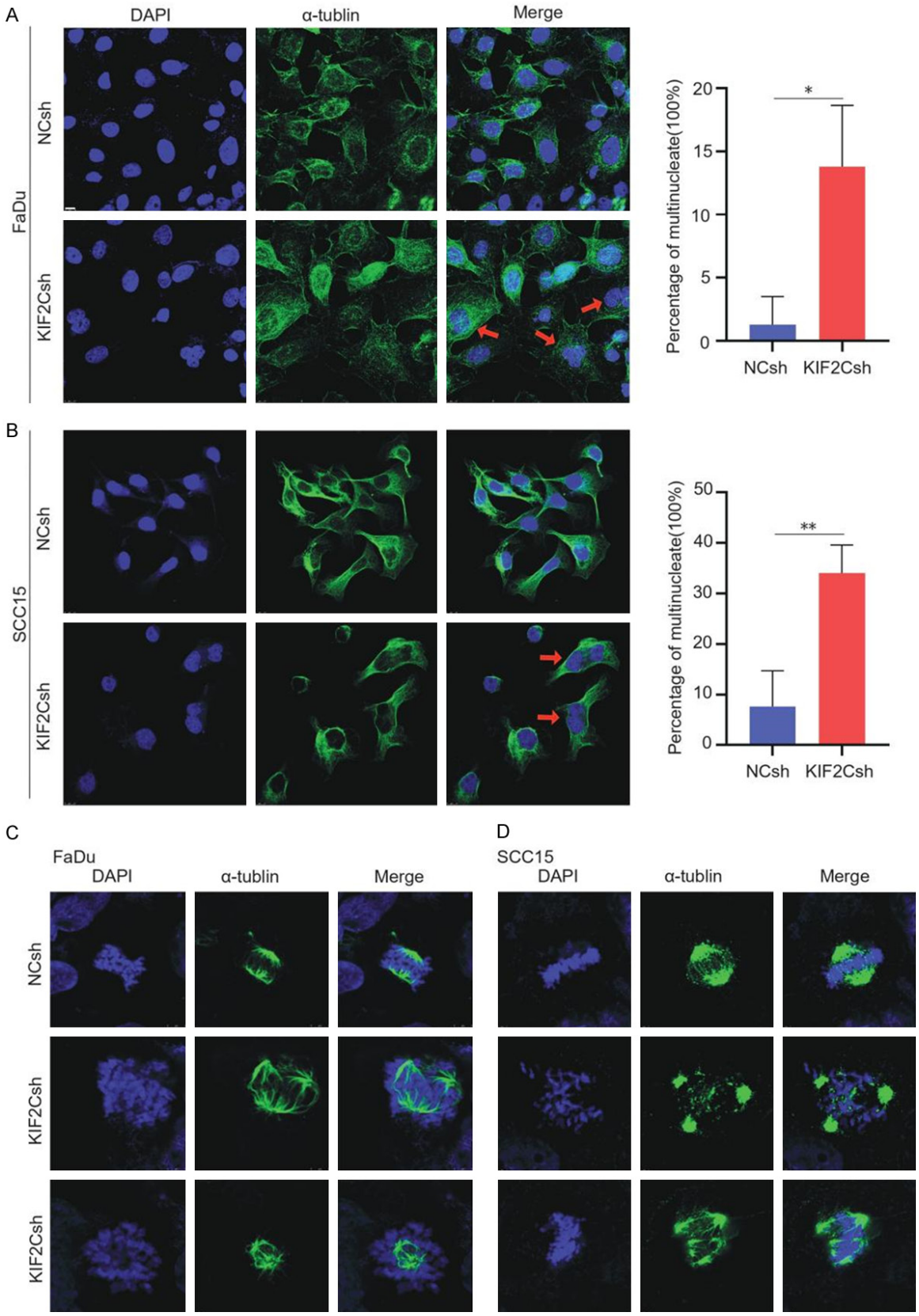

Figure 5. KIF2C silencing induces mitotic defects in HNSCC cell. (A, B) Binuclear cells and multinucleated cells were significantly increased in KIF2C knockdown cells. The cells were infected with lentivirus particles expressing nega-

tive control (NC) shRNA and KIF2C shRNA. After 36 h incubation, the fixed cells were stained with DAPI. Representative images are shown. The number of normal and defective HNSCC cells in multiple fields of view was counted under confocal microscopy, and the percentage of defective cells is shown in a histogram. Bar = 10 μm. (C, D) KIF2C knockdown induces spindle abnormalities during mitosis. The procedure for immunofluorescence was the same as in (A). SCC15 cells were blocked in G2 with Cdk1 inhibitor RO-3306 and photographed after release to record the mitotic state of the cells. Bar = 5 μm.

and Table S7). In addition, gene set enrichment analysis was performed using GSEA-4.0.3V, and a number of cancer-related gene sets were enriched (**Figure 7D**), including KRAS-activated genes, ERBB2-activated genes (ERBB2_UP.V1_UP) and EGFR-activated genes (EGFR_UP.V1_UP) (**Figure 7D**). A number of key downstream genes of KIF2C were confirmed by RT-PCR, such as KRT5, KRT14, NIT1, NID1 and TP63, PDGFA, CCNA1, RRM1, CCND2, CAV1, EGFR, SNAI2 (**Figure 7E**). In addition, KIF2C knockdown reduced the phosphorylation of AKT and ERK1/2 (**Figure 7F**). These results suggest that KIF2C may be a critical regulator of several cancer-related signaling pathways in HNSCC cells.

Therapeutic and prognostic values of KIF2C in HNSCC

Our group previously reported on the in vivo effects of KIF2C on Nasopharyngeal Carcinoma, while its role in HNSCC remains unclear. Protein expression levels of HNSCC samples from the UALCAN database show that KIF2C protein expression levels were significantly elevated in HNSCC versus normal samples (**Figure 8A**). And the HNSCC samples derived from the clinic patients validated the elevated mRNA and protein expression levels of KIF2C (**Figure 8B** and **8C**).

As shown in **Figure 8D**, KIF2C knockdown significantly reduced tumor growth in nude mice compared to the control group, indicating that KIF2C is essential for tumor growth in HNSCC.

We then assessed the prognostic significance of the top 12 key genes in the core PPI network in HNSCC patients. In the correlation heatmap of 12 key genes and 7 downstream transcription factors with transcriptomic data from clinical samples, tumor samples showed high expression of the gene targets (**Figure 8E**). The study found that the top 12 key genes are not associated with overall survival in HNSCC patients (Figure S1). Multigene combined prognostic analysis of KIF2C and transcription factors showed that the combined expression levels of KIF2C+MYBL2 and KIF2C+SP1 were prognostic for patients with head and neck squamous carcinoma (Figure S2). Our previous research has reported that KIF2C is a target of B-Myb in Lung cancer [36]. Our results also showed that the mRNA expression level of KIF2C decreased after B-Myb knockdown in HNSCC (**Figure 8F**). Specifically, our findings indicate that high expression of KIF2C with B-Myb (MYBL2) is associated with poor survival in HNSCC (**Figure 8G**). Taken together, our results suggest that KIF2C and B-Myb may be important prognostic factors in HNSCC development. These results suggest that KIF2C may have a potential therapeutic role in the HNSCC treatment.

Discussion

Our study shows that KIF2C is overexpressed in HNSCC and that this overexpression is associated with advanced clinical stage, lymphatic metastasis, and poor prognosis in HNSCC patients. Our previous studies have also reported up-regulation of KIF2C in Nasopharyngeal carcinoma [26, 30, 37, 38]. These findings suggest that KIF2C may be a crucial oncogenic gene and a potential target for HNSCC therapy.

Microtubules are non-equilibrium polymers composed of α/β-tubulin heterodimers [39]. They are essential for cell polarity, polarized cell migration, and chromosome separation during mitosis [40-42]. KIF2C is a crucial member of the kinesin 13 family that can bind to both the positive and negative ends of microtubules in vitro. It is believed that KIF2C binding to the MT terminal accelerates the transformation of microtubule dynamics by reducing the lateral interaction between fibrils [43]. Therefore, it is speculated that KIF2C plays a significant role in cell proliferation and migration. Knockdown of KIF2C in HNSCC cells results in spindle assembly abnormalities during the S phase of mitosis and inhibits cell cycle progression, proliferation, and motility. Consequently, KIF2C knockdown inhibits tumor growth in in vivo experiments. The results indicate that KIF2C plays a crucial role as an

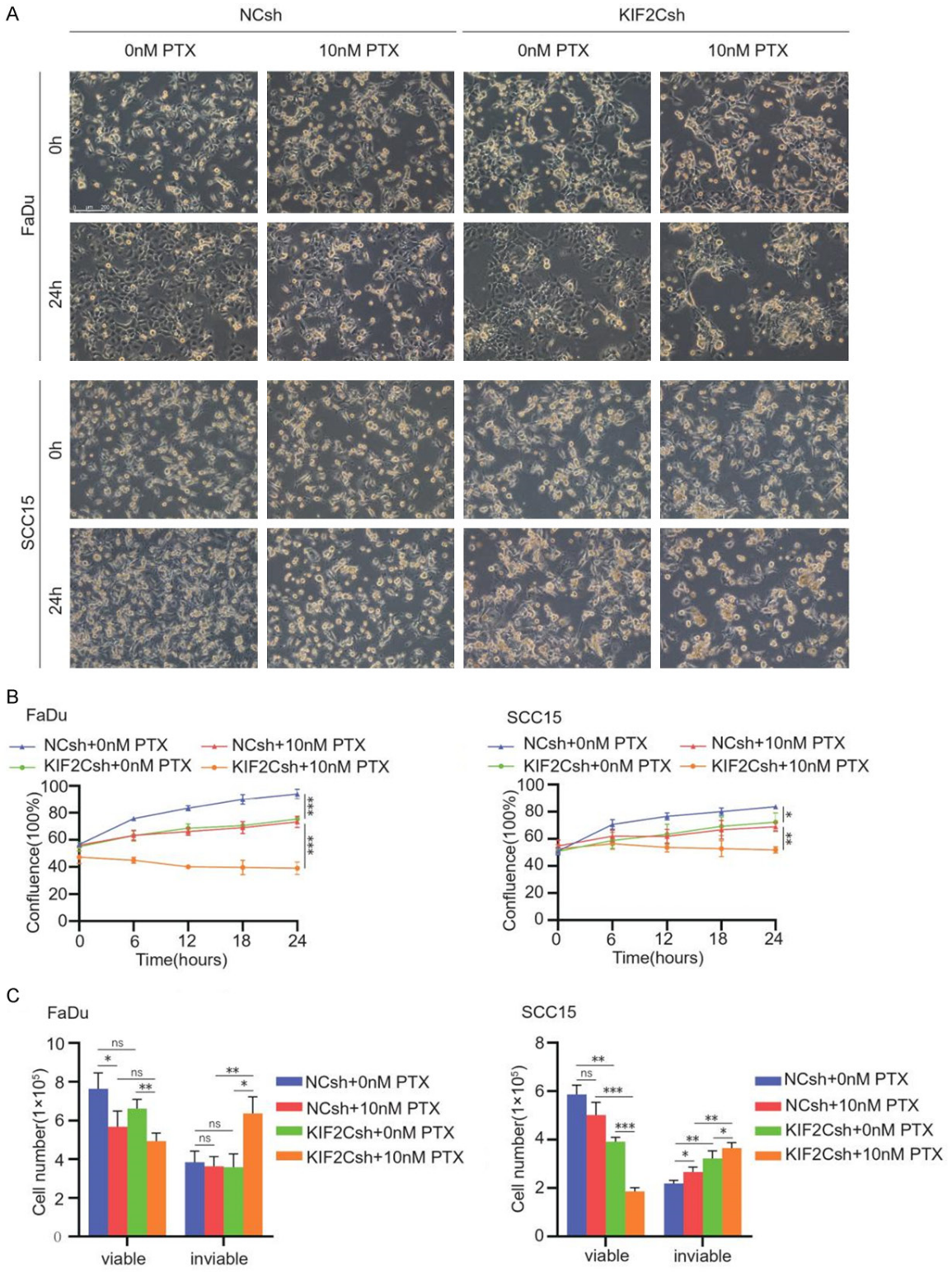

Figure 6. KIF2C knockdown enhances the effect of paclitaxel in HNSCC cells. After infected with KIF2C shRNA lentivirus for 24 h, paclitaxel (10 nM) were added to the medium. The confluency of the cells was recorded by microscope (×100) (A). With real-time imaging microscopy, cell morphology, cell growth were monitored (B). Desktop blue staining of tumor cells in mitotic phase after synchronization stains dead cells, so we counted the ratio of dead to live cells in multiple random fields of view (C). Bar = 200 μm.

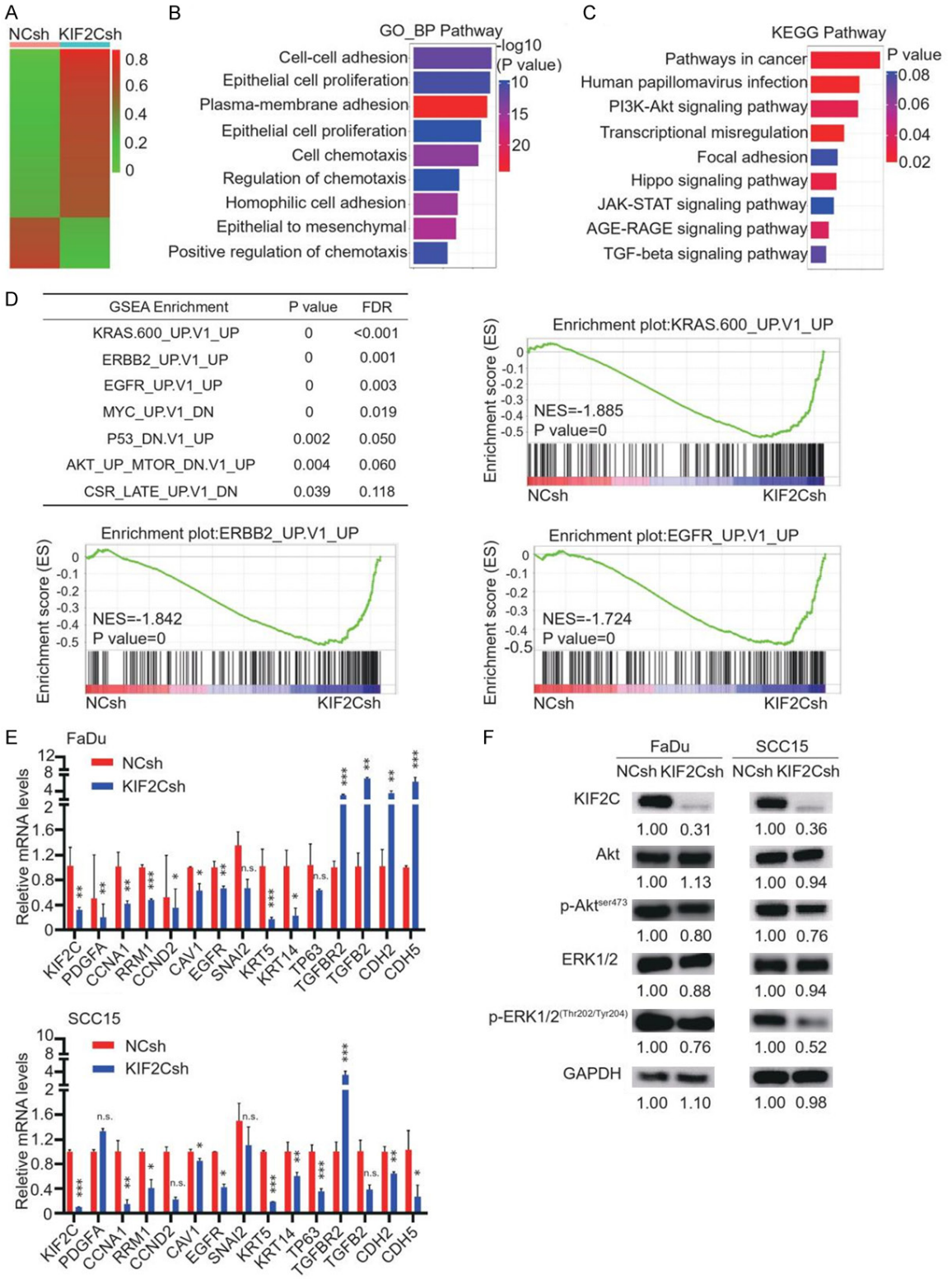

Figure 7. Downstream target genes and pathways regulated by KIF2C. A. RNA-seq was used for analysis the target genes of KIF2C. Heatmaps showed the differentially expressed genes in RNA-seq with fold change of expression more than 2.0. B, C. GO and KEGG analysis of the differentially expressed genes. D. GSEA plots of KRAS-activated genes, ERBB2-activated genes (ERBB2_UP.V1_UP) and EGFR-activated genes (EGFR_UP.V1_UP) associated with KIF2C knockdown. E. Identification of target genes regulated by KIF2C by using qRT-PCR. F. Immunoblotting detection of phosphorylation of AKT, ERK in KIF2C knockdown FaDu cells.

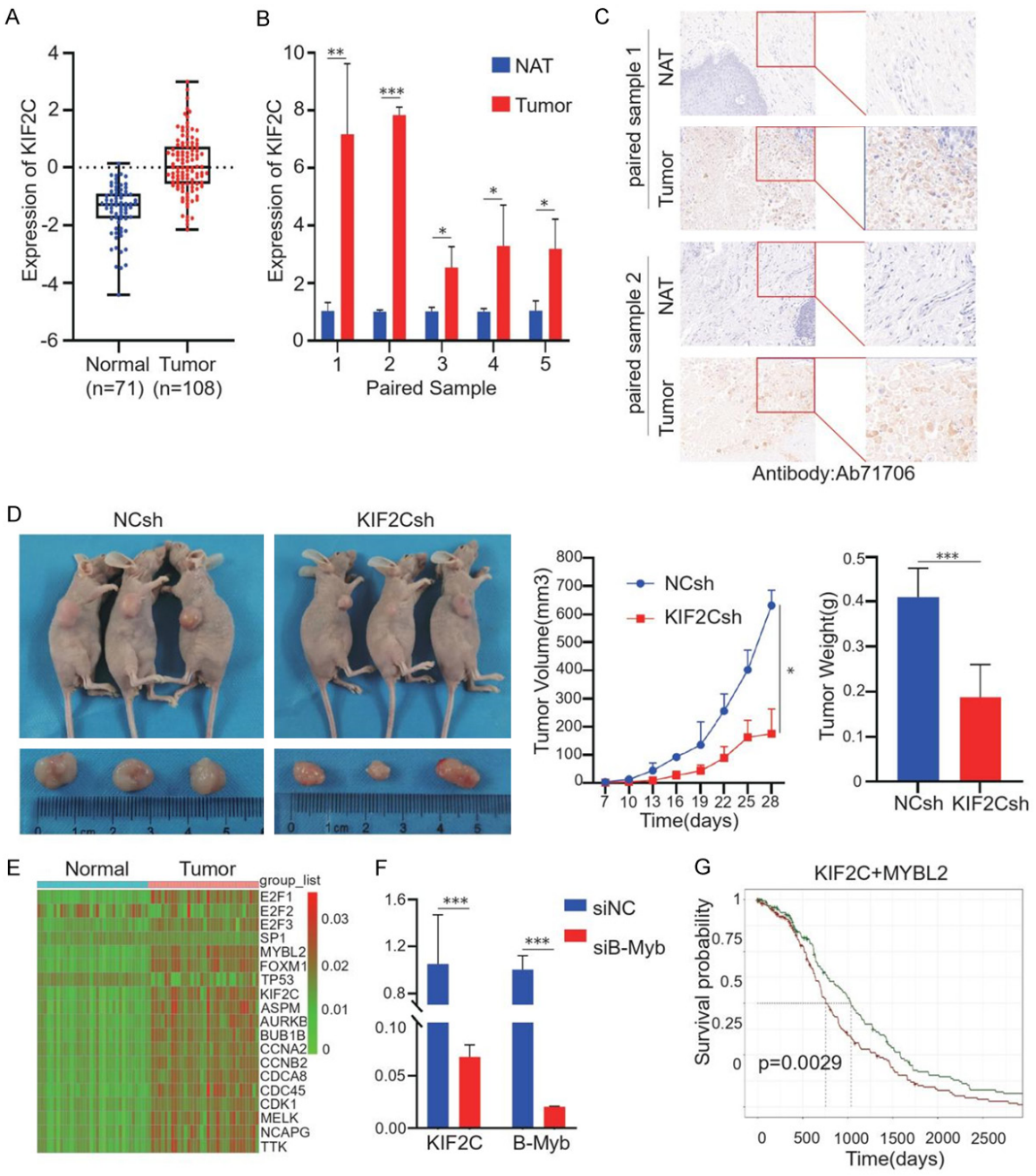

Figure 8. Therapeutic and prognostic values of KIF2C in HNSCC. A. KIF2C protein expression in HNSCC. Protein expression data are from the UALCAN database, then divided into two groups by normal tissue and tumor samples for t-test analysis. B, C. qPCR and immunohistochemical analysis of KIF2C expression in clinical samples of HNSCC. D. KIF2C silencing inhibit tumor growth in nude mouse. KIF2C knockdown FaDu cells were injected subcutaneously into the axilla of nude mice. The tumors were monitored regularly for 28 days and excised when the experiment ended. E. Heatmap of DEGs and seven transcription factors. F. The qRT-PCR validation of mRNA expression of KIF2C after siRNA-mediated B-Myb knockdown. G. Multiple gene prognostic was analyzed in HNSCC patients. Kaplan-Meier curves of overall survival were stratified by multiple gene prognostic signature in high and low risk.

oncogenic gene in HNSCC by regulating cell cycle progression, proliferation, and migration. Therefore, it may serve as a potential diagnostic and therapeutic target for HNSCC patients.

Paclitaxel promotes microtubule assembly by binding to the β-subunit of microtubules, inducing multipolar spindle division, and suppressing cell mitosis through tubulin polymerization [44,

45]. It is a recommended drug for patients with stage III-IV HNSCC [46-48]. However, its use is limited due to dose-dependent resistance and toxicity [49]. We investigated whether combining siRNA-mediated knockdown of KIF2C with paclitaxel would enhance the treatment of HNSCC patients, given KIF2C's role in regulating microtubule dynamics. Studies have shown that this combination significantly inhibits HNSCC cell proliferation. Knocking down KIF2C enhances the toxic response of HNSCC cells to paclitaxel, thereby increasing its efficacy at the same dose. In conclusion, our study indicates that the combination of KIF2C siRNA and Paclitaxel may be a promising therapeutic option for HNSCC patients with high KIF2C expression.

In the present study, phosphorylation of AKT, and ERK decreased after KIF2C knockdown. RNA-seq and RT-PCR confirmed significant changes in several downstream target genes associated with AKT or ERK. The results indicate that KIF2C has a regulatory role in the AKT or ERK signaling pathways. To investigate the role of KIF2C in vivo, we plan to construct a PDX model using tumor samples from clinical surgery and a lymphatic metastasis model. This will enable us to examine the effect of KIF2C on the malignant progression of HNSCC in vivo. These will provide more preliminary evidence for KIF2C as a therapeutic target for HNSCC treatment.

In conclusion, our study has determined that KIF2C plays a crucial role in the malignant progression of HNSCC by regulating various downstream genes and cancer-associated pathways. Therefore, it may serve as a promising therapeutic target in HNSCC.

Acknowledgements

We sincerely thank Yan Li from Southwest University for providing technical support for fluorescence microscopy. This work was supported in part by grants from the National Natural Science Foundation of China (No. 81902824 to YW), the Chongqing Municipal Science and Technology Commission (No. CSTB-2022NSCQ-MSX0885 to YW and No. 2019-0119/X1-2505 to JZ), and the Future Medical Youth Innovation Team Development Support Plan of Chongqing Medical University (W0143 to YB).

Disclosure of conflict of interest

None.

Address correspondence to: Jiang Zhu, Department of Otolaryngology, The First Affiliated Hospital of Chongqing Medical University, Chongqing Medical University, Yixueyuan Road, 1# Yuzhong District, Chongqing 400016, P. R. China. E-mail: 201959@hospital.cqmu.edu.cn; Yitao Wang, Department of Biochemistry and Molecular Biology, Chongqing Medical University, 2# Yixueyuan Road, Yuzhong District, Chongqing 400016, P. R. China. E-mail: wytao8899@cqmu.edu.cn

References

[1] Mehanna H, Paleri V, West CM and Nutting C. Head and neck cancer - Part 1: epidemiology, presentation, and prevention. BMJ 2010; 341: c4684.

[2] Sung H, Ferlay J, Siegel RL, Laversanne M, Soerjomataram I, Jemal A and Bray F. Global cancer statistics 2020: GLOBOCAN estimates of incidence and mortality worldwide for 36 cancers in 185 countries. CA Cancer J Clin 2021; 71: 209-249.

[3] Vos T, Abajobir AA, Abate KH, et al. Global, regional, and national incidence, prevalence, and years lived with disability for 328 diseases and injuries for 195 countries, 1990-2016: a systematic analysis for the Global Burden of Disease Study 2016. Lancet 2017; 390: 1211-1259.

[4] Sturgis EM and Cinciripini PM. Trends in head and neck cancer incidence in relation to smoking prevalence: an emerging epidemic of human papillomavirus-associated cancers? Cancer 2007; 110: 1429-1435.

[5] Cohen N, Fedewa S and Chen AY. Epidemiology and demographics of the head and neck cancer population. Oral Maxillofac Surg Clin North Am 2018; 30: 381-395.

[6] Mody MD, Rocco JW, Yom SS, Haddad RI and Saba NF. Head and neck cancer. Lancet 2021; 398: 2289-2299.

[7] Iocca O, Farcomeni A, Di Rocco A, Di Maio P, Golusinski P, Pardiñas López S, Savo A, Pellini R and Spriano G. Locally advanced squamous cell carcinoma of the head and neck: a systematic review and Bayesian network meta-analysis of the currently available treatment options. Oral Oncol 2018; 80: 40-51.

[8] Mesia R, Iglesias L, Lambea J, Martínez-Trufero J, Soria A, Taberna M, Trigo J, Chaves M, García-Castaño A and Cruz J. SEOM clinical guidelines for the treatment of head and neck cancer (2020). Clin Transl Oncol 2021; 23: 913-921.

[9] Kitamura N, Sento S, Yoshizawa Y, Sasabe E, Kudo Y and Yamamoto T. Current trends and future prospects of molecular targeted therapy in head and neck squamous cell carcinoma. Int J Mol Sci 2020; 22: 240.
[10] Straube A. How to measure microtubule dynamics? Methods Mol Biol 2011; 777: 1-14.
[11] Wordeman L and Mitchison TJ. Identification and partial characterization of mitotic centromere-associated kinesin, a kinesin-related protein that associates with centromeres during mitosis. J Cell Biol 1995; 128: 95-104.
[12] Andrews PD, Ovechkina Y, Morrice N, Wagenbach M, Duncan K, Wordeman L and Swedlow JR. Aurora B regulates MCAK at the mitotic centromere. Dev Cell 2004; 6: 253-268.
[13] Kline-Smith SL, Khodjakov A, Hergert P and Walczak CE. Depletion of centromeric MCAK leads to chromosome congression and segregation defects due to improper kinetochore attachments. Mol Biol Cell 2004; 15: 1146-1159.
[14] Moore AT, Rankin KE, von Dassow G, Peris L, Wagenbach M, Ovechkina Y, Andrieux A, Job D and Wordeman L. MCAK associates with the tips of polymerizing microtubules. J Cell Biol 2005; 169: 391-397.
[15] Desai A, Verma S, Mitchison TJ and Walczak CE. Kin I kinesins are microtubule-destabilizing enzymes. Cell 1999; 96: 69-78.
[16] Hunter AW, Caplow M, Coy DL, Hancock WO, Diez S, Wordeman L and Howard J. The kinesin-related protein MCAK is a microtubule depolymerase that forms an ATP-hydrolyzing complex at microtubule ends. Mol Cell 2003; 11: 445-457.
[17] Newton CN, Wagenbach M, Ovechkina Y, Wordeman L and Wilson L. MCAK, a Kin I kinesin, increases the catastrophe frequency of steady-state HeLa cell microtubules in an ATP-dependent manner in vitro. FEBS Lett 2004; 572: 80-84.
[18] Garcin C and Straube A. Microtubules in cell migration. Essays Biochem 2019; 63: 509-520.
[19] Wehrle-Haller B and Imhof BA. Actin, microtubules and focal adhesion dynamics during cell migration. Int J Biochem Cell Biol 2003; 35: 39-50.
[20] Ritter A, Kreis NN, Louwen F, Wordeman L and Yuan J. Molecular insight into the regulation and function of MCAK. Crit Rev Biochem Mol Biol 2015; 51: 228-245.
[21] Ems-McClung SC and Walczak CE. Kinesin-13s in mitosis: key players in the spatial and temporal organization of spindle microtubules. Semin Cell Dev Biol 2010; 21: 276-282.
[22] Steblyanko Y, Rajendraprasad G, Osswald M, Eibes S, Jacome A, Geley S, Pereira AJ, Maiato H and Barisic M. Microtubule poleward flux in human cells is driven by the coordinated action of four kinesins. EMBO J 2020; 39: e105432.
[23] Nakamura Y, Tanaka F, Haraguchi N, Mimori K, Matsumoto T, Inoue H, Yanaga K and Mori M. Clinicopathological and biological significance of mitotic centromere-associated kinesin overexpression in human gastric cancer. Br J Cancer 2007; 97: 543-549.
[24] Ishikawa K, Kamohara Y, Tanaka F, Haraguchi N, Mimori K, Inoue H and Mori M. Mitotic centromere-associated kinesin is a novel marker for prognosis and lymph node metastasis in colorectal cancer. Br J Cancer 2008; 98: 1824-1829.
[25] Bie L, Zhao G, Wang YP and Zhang B. Kinesin family member 2C (KIF2C/MCAK) is a novel marker for prognosis in human gliomas. Clin Neurol Neurosurg 2012; 114: 356-360.
[26] Shimo A, Tanikawa C, Nishidate T, Lin ML, Matsuda K, Park JH, Ueki T, Ohta T, Hirata K, Fukuda M, Nakamura Y and Katagiri T. Involvement of kinesin family member 2C/mitotic centromere-associated kinesin overexpression in mammary carcinogenesis. Cancer Sci 2008; 99: 62-70.
[27] Wang CQ, Xiang FG, Li YJ, Xing XM, Wang N, Chi JH and Yu WJ. Relation between the expression of mitotic centromere-associated kinesin and the progression of squamous cell carcinoma of the tongue. Oral Surg Oral Med Oral Pathol Oral Radiol 2014; 117: 353-360.
[28] Gan H, Lin L, Hu N, Yang Y, Gao Y, Pei Y, Chen K and Sun B. KIF2C exerts an oncogenic role in nonsmall cell lung cancer and is negatively regulated by miR-325-3p. Cell Biochem Funct 2019; 37: 424-431.
[29] Jiang CF, Xie YX, Qian YC, Wang M, Liu LZ, Shu YQ, Bai XM and Jiang BH. TBX15/miR-152/KIF2C pathway regulates breast cancer doxorubicin resistance via promoting PKM2 ubiquitination. Cancer Cell Int 2021; 21: 542.
[30] Zuo X, Meng P, Bao Y, Tao C, Wang Y, Liu X, Bu Y and Zhu J. Cell cycle dysregulation with overexpression of KIF2C/MCAK is a critical event in nasopharyngeal carcinoma. Genes Dis 2023; 10: 212-227.
[31] Boeckx C, Op de Beeck K, Wouters A, Deschoolmeester V, Limame R, Zwaenepoel K, Specenier P, Pauwels P, Vermorken JB, Peeters M, Van Camp G, Baay M and Lardon F. Overcoming cetuximab resistance in HNSCC: the role of AURKB and DUSP proteins. Cancer Lett 2014; 354: 365-377.
[32] Huang M, Feng X, Su D, Wang G, Wang C, Tang M, Paulucci-Holthauzen A, Hart T and Chen J. Genome-wide CRISPR screen uncovers a synergistic effect of combining Haspin and Aurora

kinase B inhibition. Oncogene 2020; 39: 4312-4322.
[33] Zhang C, Gao W, Wen S, Wu Y, Fu R, Zhao D, Chen X and Wang B. Potential key molecular correlations in laryngeal squamous cell carcinoma revealed by integrated analysis of mRNA, miRNA and lncRNA microarray profiles. Neoplasma 2016; 63: 888-900.
[34] Zhang J, Lin H, Jiang H, Jiang H, Xie T, Wang B, Huang X, Lin J, Xu A, Li R, Zhang J and Yuan Y. A key genomic signature associated with lymphovascular invasion in head and neck squamous cell carcinoma. BMC Cancer 2020; 20: 266.
[35] Wang M, Zhong B, Li M, Wang Y, Yang H and Du K. Identification of potential core genes and pathways predicting pathogenesis in head and neck squamous cell carcinoma. Biosci Rep 2021; 41: BSR20204148.
[36] Du K, Sun S, Jiang T, Liu T, Zuo X, Xia X, Liu X, Wang Y and Bu Y. E2F2 promotes lung adenocarcinoma progression through B-Myb- and FOXM1-facilitated core transcription regulatory circuitry. Int J Biol Sci 2022; 18: 4151-4170.
[37] Yang J, Wu Z, Yang L, Jeong JH, Zhu Y, Lu J, Wang B, Wang N, Wang Y, Shen K and Li R. Characterization of Kinesin family member 2C as a proto-oncogene in cervical cancer. Front Pharmacol 2022; 12: 785981.
[38] Wei S, Dai M, Zhang C, Teng K, Wang F, Li H, Sun W, Feng Z, Kang T, Guan X, Xu R, Cai M and Xie D. KIF2C: a novel link between Wnt/β-catenin and mTORC1 signaling in the pathogenesis of hepatocellular carcinoma. Protein Cell 2021; 12: 788-809.
[39] Kavallaris M. Microtubules and resistance to tubulin-binding agents. Nat Rev Cancer 2010; 10: 194-204.
[40] Akhmanova A and Kapitein LC. Mechanisms of microtubule organization in differentiated animal cells. Nat Rev Mol Cell Biol 2022; 23: 541-558.
[41] Seetharaman S, Vianay B, Roca V, Farrugia AJ, De Pascalis C, Boëda B, Dingli F, Loew D, Vassilopoulos S, Bershadsky A, Théry M and Etienne-Manneville S. Microtubules tune mechanosensitive cell responses. Nat Mater 2022; 21: 366-377.
[42] Ganguly A, Yang H, Sharma R, Patel KD and Cabral F. The role of microtubules and their dynamics in cell migration. J Biol Chem 2012; 287: 43359-43369.
[43] Moon HH, Kreis NN, Friemel A, Roth S, Schulte D, Solbach C, Louwen F, Yuan J and Ritter A. Mitotic centromere-associated kinesin (MCAK/KIF2C) regulates cell migration and invasion by modulating microtubule dynamics and focal adhesion turnover. Cancers (Basel) 2021; 13: 5673.
[44] Salama JK, Stenson KM, Kistner EO, Mittal BB, Argiris A, Witt ME, Rosen F, Brockstein BE, Cohen EE, Haraf DJ and Vokes EE. Induction chemotherapy and concurrent chemoradiotherapy for locoregionally advanced head and neck cancer: a multi-institutional phase II trial investigating three radiotherapy dose levels. Ann Oncol 2008; 19: 1787-1794.
[45] Zhao S, Tang Y, Wang R and Najafi M. Mechanisms of cancer cell death induction by paclitaxel: an updated review. Apoptosis 2022; 27: 647-667.
[46] Vermorken JB, Remenar E, van Herpen C, Gorlia T, Mesia R, Degardin M, Stewart JS, Jelic S, Betka J, Preiss JH, van den Weyngaert D, Awada A, Cupissol D, Kienzer HR, Rey A, Desaunois I, Bernier J and Lefebvre JL; EORTC 24971/TAX 323 Study Group. Cisplatin, fluorouracil, and docetaxel in unresectable head and neck cancer. N Engl J Med 2007; 357: 1695-1704.
[47] Posner MR, Hershock DM, Blajman CR, Mickiewicz E, Winquist E, Gorbounova V, Tjulandin S, Shin DM, Cullen K, Ervin TJ, Murphy BA, Raez LE, Cohen RB, Spaulding M, Tishler RB, Roth B, Viroglio Rdel C, Venkatesan V, Romanov I, Agarwala S, Harter KW, Dugan M, Cmelak A, Markoe AM, Read PW, Steinbrenner L, Colevas AD, Norris CM Jr and Haddad RI; TAX 324 Study Group. Cisplatin and fluorouracil alone or with docetaxel in head and neck cancer. N Engl J Med 2007; 357: 1705-1715.
[48] Hitt R, López-Pousa A, Martínez-Trufero J, Escrig V, Carles J, Rizo A, Isla D, Vega ME, Martí JL, Lobo F, Pastor P, Valentí V, Belón J, Sánchez MA, Chaib C, Pallarés C, Antón A, Cervantes A, Paz-Ares L and Cortés-Funes H. Phase III study comparing cisplatin plus fluorouracil to paclitaxel, cisplatin, and fluorouracil induction chemotherapy followed by chemoradiotherapy in locally advanced head and neck cancer. J Clin Oncol 2005; 23: 8636-8645.
[49] Rajendra A, Noronha V, Joshi A, Patil VM, Menon N and Prabhash K. Palliative chemotherapy in head and neck cancer: balancing between beneficial and adverse effects. Expert Rev Anticancer Ther 2020; 20: 17-29.

Table S1. List of shRNA sequences

Gene name	Primer name and sequences
Negative control shRNA (NCsh)	Sense: 5'-ACCGGTTGGTTTACATGTTGTGTGACTCGAG TCACACAACATGTAAAC-CATTTTT-3'
	Antisense: 5'-GAATTCAAAAATGGTTTACATGTTGTGTGACTCGAG TCACACAACATGTA-AACCA-3'
KIF2C shRNA (KIF2Csh)	Sense: 5'-ACCGGTCGCCCACTGAATAAGCAAGAACTCGAGTTCTTGCTTATTCAGTGGGC-GTTTTT-3'
	Antisense: 5'-GAATTCAAAAACGCCCACTGAATAAGCAAGAACTCGAGTTCTTGCT-TATTCAGTGGGCG-3'

Table S2. List of primer sequences used for qRT-PCR analysis

Gene name	Primer name and sequences
GAPDH	F833: 5'-ACCTGACCTGCCGTCTAGAA-3'
	R1060: 5'-TCCACCACCCTGTTGCTGTA-3'
KIF2C	F945: 5'-CTACAGGTTCACAGCAAGGC-3'
	R1148: 5'-TTCCGGTAGCAGGGTTGATT-3'
KRT14	F839: 5'-TGAGCCGCATTCTGAACGAG-3'
	R1313: 5'-GATGACTGCGATCCAGAGGA-3'
KRT5	F872: 5'-CCAAGGTTGATGCACTGATGG-3'
	R961: 5'-TGTCAGAGACATGCGTCTGC-3'
SNAI2	F60: 5'-CGAACTGGACACACATACAGTG-3'
	R146: 5'-CTGAGGATCTCTGGTTGTGGT-3'
TP63	F360: 5'-GGACCAGCAGATTCAGAACGG-3'
	R541: 5'-AGGACACGTCGAAACTGTGC-3'
EGFR	F795: 5'-CCCACTCATGCTCTACAACCC-3'
	R989: 5'-TCGCACTTCTTACACTTGCGG-3'
CAV1	F68: 5'-GCGACCCTAAACACCTCAAC-3'
	R158: 5'-ATGCCGTCAAAACTGTGTGTC-3'
ICAM1	F77: 5'-ATGCCCAGACATCTGTGTCC-3'
	R188: 5'-GGGGTCTCTATGCCCAACAA-3'
ITGB2	F55: 5'-TGCGTCCTCTCTCAGGAGTG-3'
	R241: 5'-GGTCCATGATGTCGTCAGCC-3'
CDH2	F578: 5'-TGCGGTACAGTGTAACTGGG-3'
	R700: 5'-GAAACCGGGCTATCTGCTCG-3'
CDH5	F219: 5'-AAGCGTGAGTCGCAAGAATG-3'
	R397: 5'-TCTCCAGGTTTTCGCCAGTG-3'
TGFBR2	F662: 5'-AAGATGACCGCTCTGACATCA-3'
	R780: 5'-CTTATAGACCTCAGCAAAGCGAC-3'
FN1	F393: 5'-GAGAATAAGCTGTACCATCGCAA-3'
	R592: 5'-CGACCACATAGGAAGTCCCAG-3'
RRM1	F235: 5'-GCCAGGATCGCTGTCTCTAAC-3'
	R340: 5'-GAGAGTGTTTGCCATTATGTGGA-3'
CCNA1	F182: 5'-GAGGTCCCGATGCTTGTCAG-3'
	R263: 5'-GTTAGCAGCCCTAGCACTGTC-3'
TGFB2	F72: 5'-CAGCACACTCGATATGGACCA-3'
	R184: 5'-CCTCGGGCTCAGGATAGTCT-3'
CCND2	F1871: 5'-TTCATTGCAGACACCACCAT-3'
	R2082: 5'-TGTGAACCAGACATGCCAAT-3'
PDGFA	F768: 5'-ACACGAGCAGTGTCAAGTGC-3'
	R967: 5'-GGCTCATCCTCACCTCACAT-3'

Table S3. Antibodies used in the present study

Protein name	Manufacture (cat. number)	Applications (working dilution)	Website Link
GAPDH	Xianzhi Bio (AB-P-R 001)	IB (1:5000)	http://www.goodhere.com/showproduct.asp?id=320&classid=34&nid=2
KIF2C	Abcam (ab187652)	IB (1:1000)	https://www.abcam.cn/mcak-antibody-epr14838-ab187652.html
mTOR	Ruiying Bio (RLT2914)	IB (1:1000)	http://www.ruiyingbio.com/showproduct.asp?/1_4581,%E4%B8%80%E6%8A%97
p-mTOR	Ruiying Bio (RLP0176)	IB (1:1000)	http://www.ruiyingbio.com/showproduct.asp?/1_546,%E4%B8%80%E6%8A%97
Akt	Bimake (A5031)	IB (1:1000)	https://www.bimake.cn/antibody/akt1-2-3-rabbit-recombinant-mab.html
p-Akt	Bimake (A5030)	IB (1:1000)	https://www.bimake.cn/antibody/phospho-akt-ser473-rabbit-recombinant-mab.html
Tubulin	Beyotime (AT819)	IF (1:500)	https://www.beyotime.com/product/AT819.htm
Anti-Rabbit secondary antibody	Abgent (ASS1009)	IB (1:5000)	http://www.abgent.com/products/ASS1009-Goat-Anti-Rabbit-IgGHL-MouseHuman-ads-HRP-Secondary-Antibody
Anti-Mouse secondary antibody	Thermo (A-11031)	IF (1:1000)	https://www.thermofisher.com/antibody/product/Goat-anti-Mouse-IgG-H-L-Secondary-Antibody-Polyclonal/A-11031

Table S4. Top list of the GO enrichment of common DEGs in HNSCC

ID	Description	*P* value	Count
GO:0030198	Extracellular matrix organization	6.50E-27	116
GO:0007517	Muscle organ development	1.15E-16	103
GO:0008544	Epidermis development	6.60E-11	89
GO:0050900	Leukocyte migration	1.54E-09	94
GO:0022407	Regulation of cell-cell adhesion	1.13E-08	106
GO:0007492	Endoderm development	4.03E-08	30
GO:0006631	Fatty acid metabolic process	6.02E-08	93
GO:0060326	Cell chemotaxis	2.98E-07	76
GO:0071674	Mononuclear cell migration	3.22E-07	54
GO:0140014	Mitotic nuclear division	4.39E-06	68

Table S5. Top list of the KEGG pathway enrichment of common DEGs in HNSCC

ID	Description	*P* value	Count
hsa04512	ECM-receptor interaction	6.71E-11	38
hsa04510	Focal adhesion	2.22E-08	60
hsa05222	Small cell lung cancer	8.96E-06	30
hsa05165	Human papillomavirus infection	3.87E-05	75
hsa04810	Regulation of actin cytoskeleton	0.00030015	53
hsa03320	PPAR signaling pathway	0.000731855	22
hsa00590	Arachidonic acid metabolism	0.000737398	19
hsa04110	Cell cycle	0.001039136	32
hsa04630	JAK-STAT signaling pathway	0.002515833	38
hsa04151	PI3K-Akt signaling pathway	0.003813275	70

Table S6. Top list of the GO enrichment of dysregulated genes in KIF2C knockdown cells

Term ID	Description	*P* value	Count
GO:0098742	Cell-cell adhesion via plasma-membrane adhesion molecules	2.64E-11	50
GO:0050673	Epithelial cell proliferation	3.59E-05	52
GO:0050678	Regulation of epithelial cell proliferation	7.04E-05	46
GO:0001837	Epithelial to mesenchymal transition	1.13E-07	29
GO:0007156	Homophilic cell adhesion via plasma membrane adhesion molecules	3.13E-07	30
GO:0022407	Regulation of cell-cell adhesion	7.37E-06	53
GO:0060326	Cell chemotaxis	6.99E-07	44
GO:0050920	Regulation of chemotaxis	6.99E-05	31
GO:0050921	Positive regulation of chemotaxis	4.67E-05	23
GO:0098742	Cell-cell adhesion via plasma-membrane adhesion molecules	2.64E-11	50

Table S7. Top list of the KEGG enrichment of dysregulated genes in KIF2C knockdown cells

Term ID	Description	*P* value	Count
hsa05200	Pathways in cancer	0.007950504	54
hsa04390	Hippo signaling pathway	0.016645694	20
hsa04151	PI3K-Akt signaling pathway	0.02011897	37
hsa05202	Transcriptional misregulation in cancer	0.002717359	26
hsa04510	Focal adhesion	0.083641137	21
hsa04933	AGE-RAGE signaling pathway in diabetic complications	0.025733828	14
hsa05165	Human papillomavirus infection	0.004342732	38
hsa04630	JAK-STAT signaling pathway	0.085608227	18
hsa04350	TGF-beta signaling pathway	0.076551234	12
hsa05200	Pathways in cancer	0.007950504	54

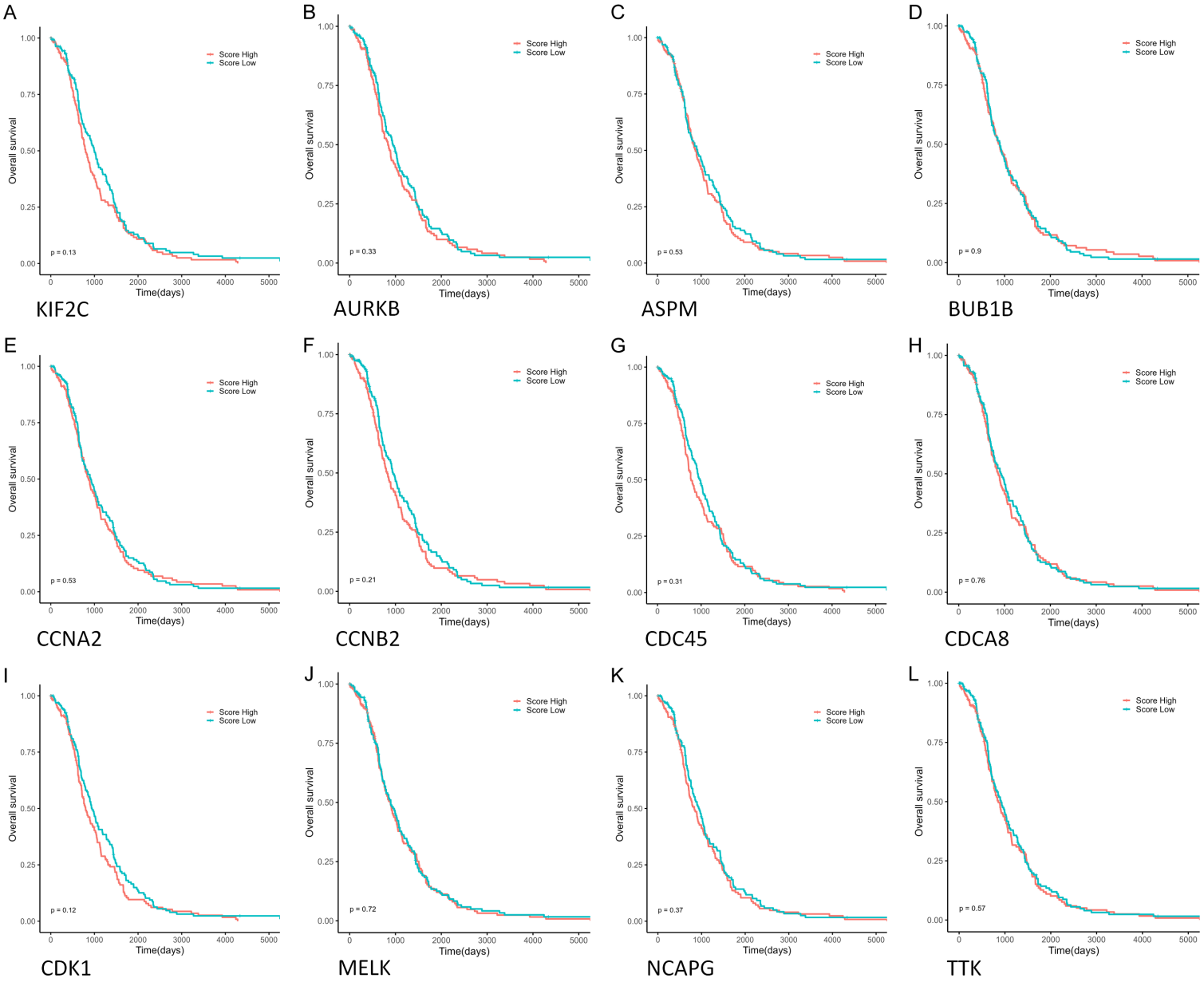

Figure S1. Survival analysis of 12 DEGs.

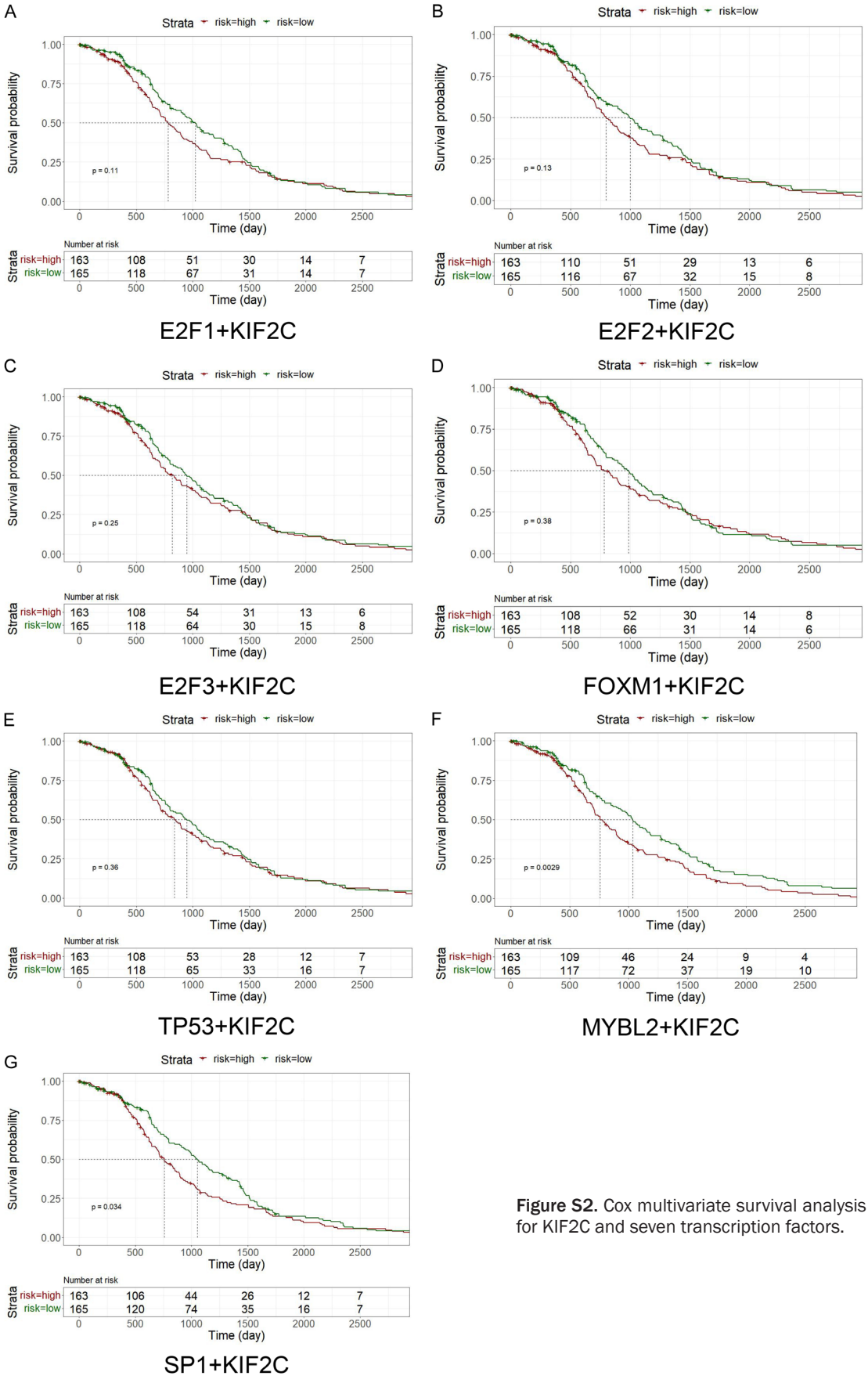

Figure S2. Cox multivariate survival analysis for KIF2C and seven transcription factors.